

STRUCTURAL FLUCTUATIONS AND THERMOPHYSICAL PROPERTIES OF MOLTEN II-VI COMPOUNDS

Ching-Hua Su^{1*}, S. Zhu², C. Li³, R. Scripa³, S. L. Lehoczky¹, Y. W. Kim⁴, J. K. Baird⁴, B. Lin³,
H. Ban³, Chris Benmore⁵, and S. Feth⁴

NASA, Marshall Space Flight Center¹, Universities Space Research Association²,
University of Alabama at Birmingham³, University of Alabama in Huntsville⁴,
National Argonne Laboratory⁵

The objectives of the project are to conduct ground-based experimental and theoretical research on the structural fluctuations and thermophysical properties of molten II-VI compounds to enhance the basic understanding of the existing flight experiments in microgravity materials science programs as well as to study the fundamental heterophase fluctuation phenomena in these melts by:

- 1) conducting neutron scattering analysis and measuring quantitatively the relevant thermophysical properties of the II-VI melts (such as viscosity, electrical conductivity, thermal diffusivity and density) as well as the relaxation characteristics of these properties to advance the understanding of the structural properties and the relaxation phenomena in these melts and
- 2) performing theoretical analyses on the melt systems to interpret the experimental results.

All the facilities required for the experimental measurements have been procured, installed and tested. It has long been recognized that liquid Te presents a unique case having properties between those of metals and semiconductors. The electrical conductivity for Te melt increases rapidly at melting point, indicating a semiconductor-metal transition. Te melts comprise two features, which are usually considered to be incompatible with each other: covalently bound atoms and metallic-like behavior. ‘Why do Te liquids show metallic behavior?’ is one of the long-standing issues in liquid metal physics. Since thermophysical properties are very sensitive to the structural variations of a melt, we have conducted extensive thermophysical measurements on Te melt.

The Torsion Oscillation Cup Method

The torsion oscillation cup method, which was employed at MSFC to measure the viscosity of HgTe, HgCdTe and HgZnTe melts is a practical method for a nonintrusive measurement of the viscosity of melts at high temperatures and under high pressures [1, 2]. The method involves the measurements of the damped oscillatory motion of a vertical cylindrical crucible containing the melt attached by means of a torsion wire. The disadvantage of the technique is that the measurement time is too long, one to two hours, to study the dynamics of phase transformations, or homogenization processes with characteristic times on the order of minutes. Sometimes it is also difficult to maintain stable test condition, especially at high temperatures. A number of factors, including drift in the physical properties of torsion wire over long time periods at elevated temperatures, can influence the precision of the method. Recently, through the NASA Advanced Technology Development (ATD) program, we have developed a novel technique to nonintrusively and simultaneously measure viscosity and electrical conductivity of metallic and semiconductor melts. The essential feature of this technique is the utilization of an axial rotating magnetic

Keywords: thermophysical and thermodynamic properties, II-VI compounds

*Corresponding author. E-mail: ching.hua.su@msfc.nasa.gov

field (RMF), as shown in Figure 4, which induces controllable fluid flows in the melt. The RMF causes a rotation of the fluid that in turn exerts a torque on the wall of the stationary enclosure. When the force inducing the fluid motion is removed, the rotation of the fluid decays and the fluid comes to rest. The characteristics of the transient torque decay can be used to calculate the fluid viscosity and the steady-state torque applied to the enclosure by a given magnetic field to calculate the melt electrical conductivity.

The rotating motion of the ampoule is measured by the angular deflection of the quartz fiber (torsion wire) as a function of time using an optical encoder (Micro-E, Inc.). An evacuated bell jar is being used to reduce noise caused by air currents and allows more reproducible and precise measurements of the angular deflection. A typical result for a HgTe sample is given in Figure 6, where the measured deflection angle is shown as a function of time. The RMF was turned on at time about 40s, then turned off at about 230s, and the ampoule was then free to rotate. Two methods were developed to analyze the data. The first one is an analytical method. The stationary torque caused by the applied RMF can be determined from the average of the deflecting angular oscillations. The electrical conductivity can be derived by comparing the torque with that of a standard sample of known electrical conductivity, such as Hg or Ga melt, sealed inside an ampoule of identical dimensions. The measured angular deflection after the RMF has been turned off is similar to that of an oscillation-cup viscometer and its logarithmic decrement can be utilized to determine the viscosity analytically by the approximate Roscoe formula [2, 3].

In the second method, the coupled equations for fluid flow and ampoule torsional vibrations were solved numerically [4]. The unknown variables, electrical conductivity and viscosity of the melt, were allowed to vary to obtain a best fit to the experimental data of deflecting angle vs. time. As seen in Figure 6, the simulation results are in a good agreement with the experimental data; the ratio difference between the experimental and calculated results is less than 10^{-4} . The transient velocity of the melt caused by the rotating magnetic field was found to reach equilibrium in about half a minute and the viscosity of melt could be determined from the magnitude of the oscillation. This allows a viscosity measurement in a minute or so, in contrast to the existing oscillation cup method, which requires at least an hour for a measurement. We have also performed measurements under identical conditions except for the various RMF running times (1 to 15 min) that were used to take the data. The numerical analysis yielded nearly identical values as those determined analytically for the electrical conductivity and viscosity. For example, the best fit, shown in Figure 6, gives a value of $3.04 \times 10^{-7} (\text{m}^2/\text{s})$ for Te melt at 470°C compared to the value of $3.1 \times 10^{-7} (\text{m}^2/\text{s})$ determined by an approximate analytical method.

The viscosity can be obtained by numerically solving the melt flow and ampoule oscillation equations simultaneously with viscosity as the adjustable parameter and fitting the solution to experimental deflection-time data. The ampoule rotational oscillation can be described as:

$$I\omega^2 \left[\frac{d^2\alpha(t)}{dt^2} + 2\Delta_0 \frac{d\alpha(t)}{dt} + (1 + \Delta_0^2)\alpha(t) \right] = M(t)$$

where the ampoule-melt interaction (torque exerted by melt flow on ampoule wall) is:

$$M(t) = -2\pi R^2 h \rho v \left. \frac{dV_\theta}{dr} \right|_{r=R}$$

The melt rotational flow under RMF is:

$$\frac{\partial V_\theta}{\partial t} = f_\theta + v \left(\frac{\partial^2 V_\theta}{\partial r^2} + \frac{1}{r} \frac{\partial V_\theta}{\partial r} - \frac{V_\theta}{r^2} \right)$$

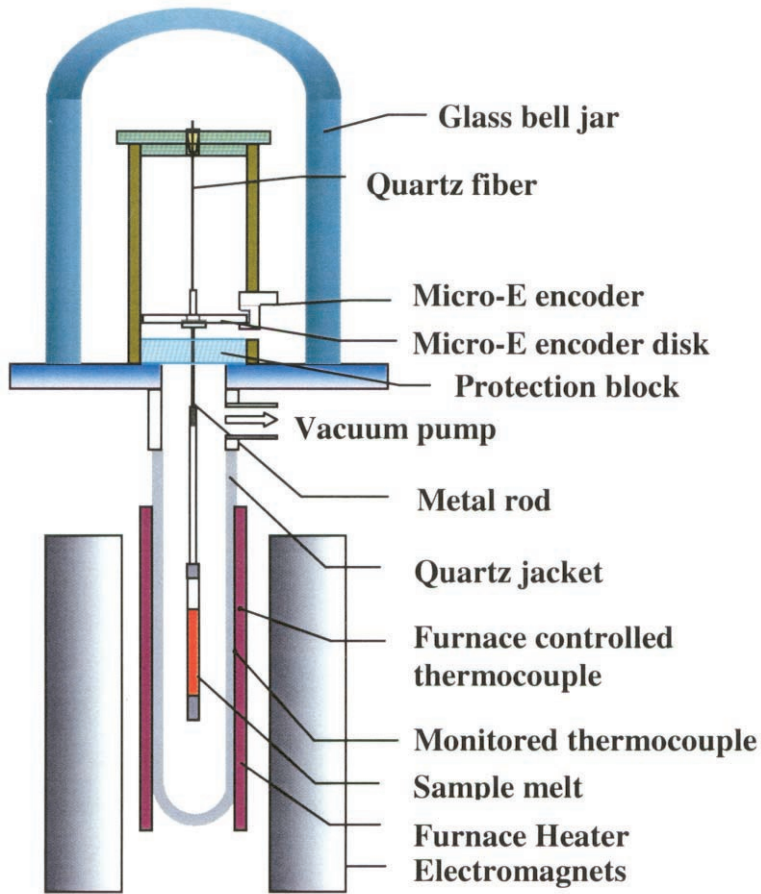


Figure 1. Schematics of the viscometer with the rotating magnetic field.

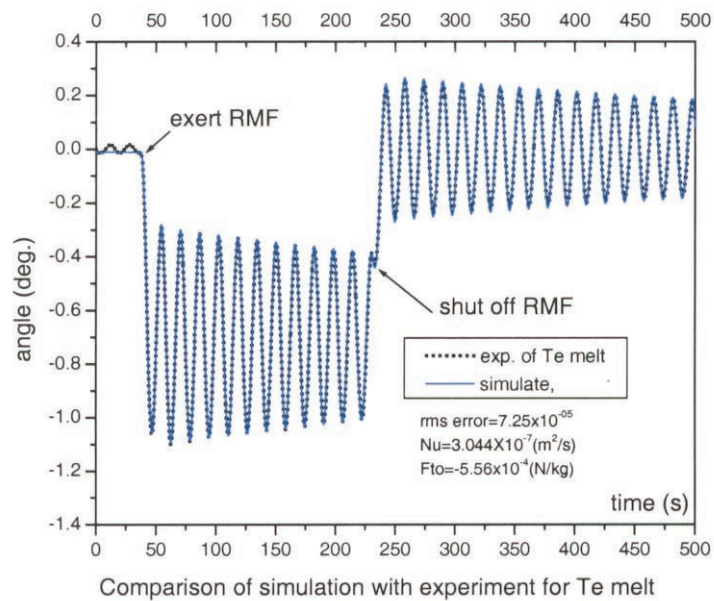


Figure 2. The angular deflection vs. time for HgTe melt. The dotted line is the experimental results and the blue solid line the calculated results

Where the Lorentz force f_g is given by:

$$f_{\theta} = f_{\theta 0} \cdot \frac{r}{R\omega_o} \left(\omega_o - \frac{V_{\theta}}{r} \right)$$

and the initial and boundary conditions are:

$$V_{\theta}(r,t)=0, \text{ when } t=0; \text{ and } V_{\theta}(R,t)=R \frac{d\alpha}{dt}$$

The electrical conductivity of the melt can be determined from the torque induced by the melt flow at equilibrium:

$$M_{eq} = \frac{\pi}{4} B_0 \sigma \omega h R^4$$

NOMENCLATURE

| | | | |
|-------|-----------------------------------|--------------|--------------------------------------|
| B_0 | magnetic induction | α | deflection angle of the ampoule |
| f_g | Lorentz force | V_{θ} | fluid rotational velocity |
| h | height of the melt in the ampoule | σ | electrical conductivity of the melt |
| I | moment of inertia of system | ω_o | angular velocity of RMF |
| M | torque induced by melt flow | ρ | density of the melt |
| R | radius of the ampoule | Δ_0 | logarithmic decrement of oscillation |
| t | time | ν | kinematic viscosity of the melt |
| r | radial coordinate | | |

The measured kinematic viscosity of Te melt as a function of temperature as shown in Figure 3. Comparing with the previous results [5] our data are generally low by about 10%. However, the most prominent feature of our data, which was not reported before, is the sharp peak of viscosity, which was reproducibly observed in the temperature range between 500 and 560°C. The measured electrical conductivity of Te melt is given in Figure 4. Our data agree well with previous results and confirm the semiconducting-metallic transition just above the melting point.

Thermal diffusivity and heat capacity.

A dynamic measurement of thermal diffusivity using the laser flash method [6, 7] has been employed previously to determine the thermal conductivity of various composite materials as well as materials that have to be enclosed in closed ampoules due to their high vapor pressures or toxic nature. In this method, the front surface of a small disk-shaped sample positioned vertically inside a furnace is subjected to a very short burst of radiant energy from a laser pulse with a radiation time of 1ms or less. The resulting temperature rise of the rear surface of the sample is measured and thermal diffusivity calculated from the temperature rise versus time. The thermal diffusivities of $Hg_{1-x}Cd_xTe$ solids and melts [8], pure Te, Te-rich HgCdTe and Te-rich HgZnTe melts [9] were determined using this technique. Using the technique we have also measured the thermal diffusivities for $Hg_{1-x}Zn_xTe$ solids and melts [10].

During this project, we have constructed the instrumental setup for thermal diffusivity measurements as schematically shown in figure 5. A pulsed laser beam with 1064 nm wavelength was focused to 10 mm diameter and to illuminate one side of the Te melt. The laser energy variation from pulse to pulse at defined energy was 1% and the pulse duration used in experiments was 1 millisecond. An inferred CdZnTe

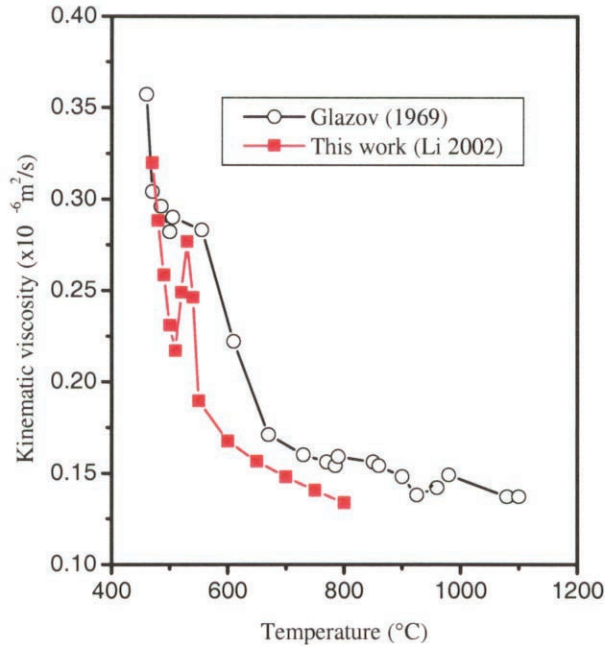


Figure 3. Measured kinematic viscosity of Te melt as a function of temperature.

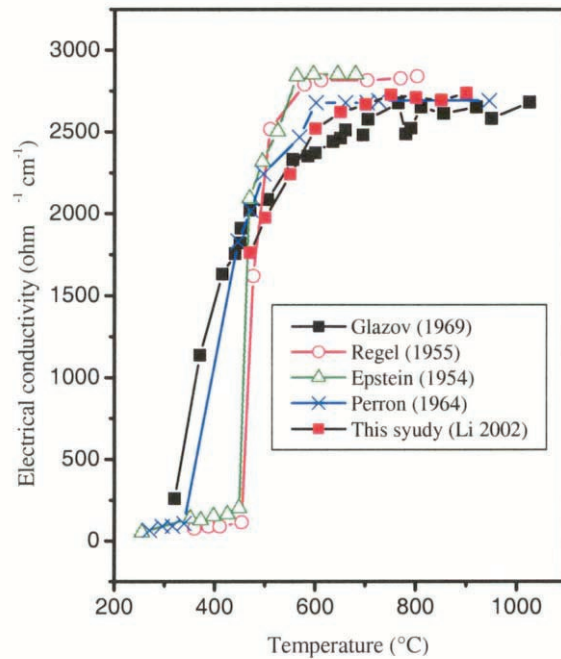


Figure 4. Measured electrical conductivity of Te melt as a function of temperature.

detector was installed at the other side of the sample cell and was focused at the sample center with a 2 mm diameter spot. The detector ranges from 723 K to 1473 K.

We can simultaneously determine the specific heat and thermal diffusivity of a sample by performing numerical simulation of overall heat transfer. Very well defined boundary conditions are required to match the experimental and simulation conditions. We are using a YAG laser for the radiation source, with a 608

spatially uniform intensity as close as possible to a delta function, and the beam diameter at the front surface of the sample cell can be adjusted to match the sample diameter.

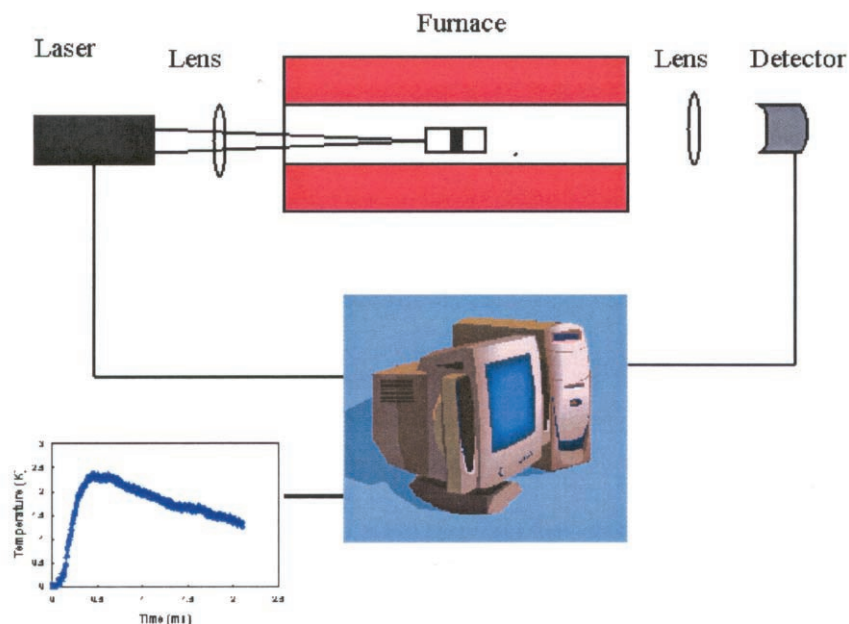


Figure 5. The schematic apparatus of laser flash measurement

Te powder was sealed in a specially designed cylindrical-shape optical quartz cell. The outer and inner diameters of the optical cell are 15 mm and 10 mm, respectively. The cell was 22 mm long and the sample thickness was about 2 mm. Sample was clamped into a stainless steel block that is placed at the center of a furnace with a heat pipe made of stainless steel. The temperature-uniform zone was about 10 cm and the variation in the measurement range was less than 0.5 K. Before making the measurements, the cell containing Te powder was first heated at 1083 K for 48 hours to ensure the Te was in a homogeneous liquid state. After reaching the steady state at measurement temperature, five thermal diffusivity measurements were performed at this temperature. Between each measurement, a 15-minute waiting period was used to let the liquid T back to same initial state. Sample was measured when it was heated up and cooled down. The radiation energy was collected and converted into temperature at 1 KHz rate. The measurement started about one second before the laser illumination and last for 10 seconds. Figure 6 shows first two-second part of a thermal diffusivity transient of Te melts at 873 K.

The specific heat of Te melt deduced from the numerical fit in the measuring temperature range is shown in figure 7. As a comparison, several curves originated from published references [11-13] are also plotted in the figure.

The thermal diffusivity data, which is shown in figure 8, are calculated from the experimental data by using an analytic method. Measurements from both rising and cooling temperature processes are plotted in this figure. The data are almost overlapped within the error range. The variation of each data point is about 3%. Thermal diffusivity data measured by Maleki and Holland [9] are also plotted in the figure 4, which agrees well with our data at low temperatures. Their measurements stopped at 923 K without any indication of the temperature-dependent at high temperatures. Our experiment data show that a similar

linear temperature-dependent of thermal diffusivity extended to 1023 K. After this temperature, however, the thermal diffusivity keeps at a nearly constant value.

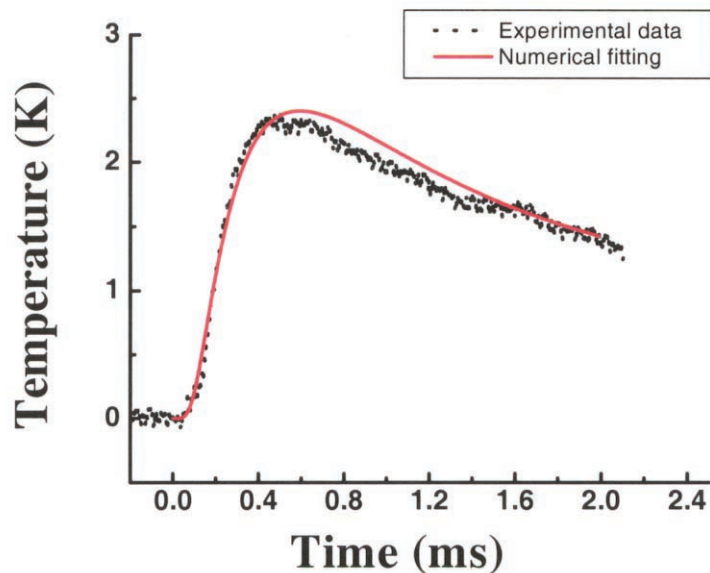


Figure 6. Temperature transient curves of liquid Te at 873 K, (dot line) experimental measurement and (solid line) numerical fitting.

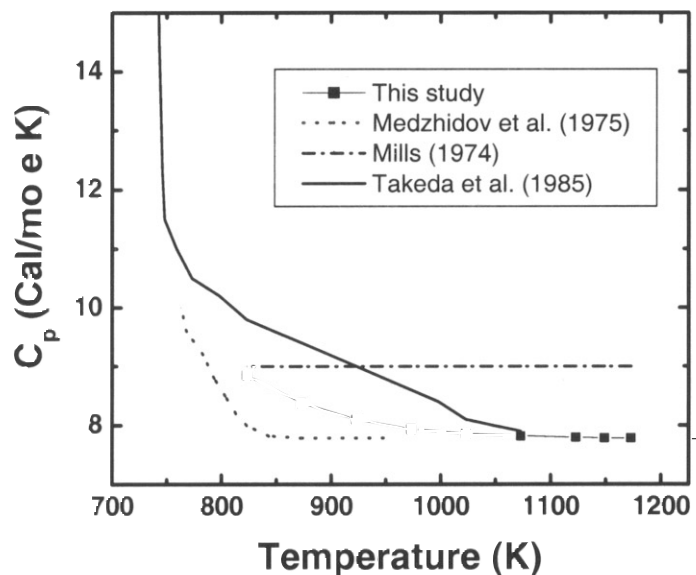


Figure 7. Specific heat curve of liquid Te as a function of temperature.

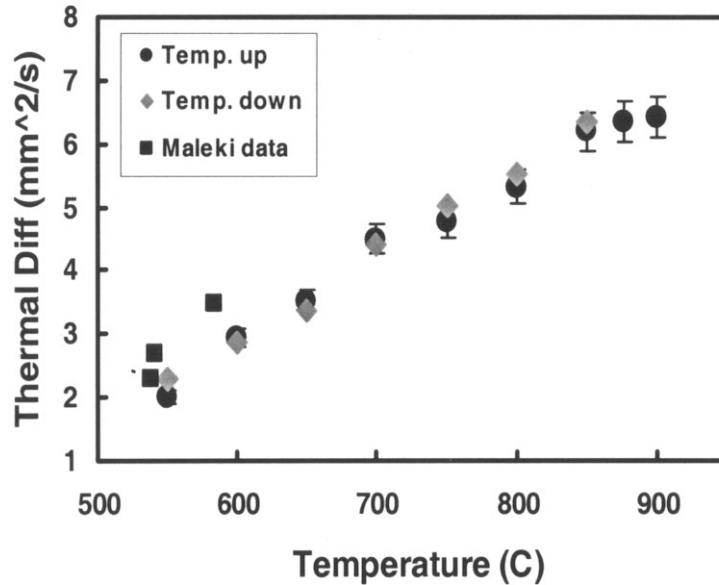


Figure 8. Thermal diffusivity vs. temperature for liquid Te

References

1. Mazuruk, K. (1995), Ching-Hua Su, S. L. Lehoczky and F. Rosenberger, *J. Appl. Phys.* 77 5098.
2. Mazuruk, K. (1996), Ching-Hua Su, Yi-Gao Sha and S. L. Lehoczky, *J. Appl. Phys.* 79 9080.
3. Roscoe, R. (1963), *Proc. Phys. Soc. London* 72 576.
4. Lin, B. (2002), Chao Li, Heng Ban, Rose Scripa, Shen Zhu, Ching-Hua Su, and S. L. Lehoczky, to be presented at 2002 ASME (International Mechanical Engineering Congress and Exposition), New Orleans November 17-22, 2002.
5. Glazov, V. M. (1969), S. N. Chizhevskaya and N. N. Glagoleva, "Liquid Semiconductors", Plenum Press, New York.
6. Parker, W. J. (1961), R. J. Jenkins, C. P. Butler and G. L. Abbott, *J. Appl. Phys.* 32 1679.
7. Taylor, R. E. (1979), *High Temp.-High Pressures* 11 43.
8. Holland, L. R. (1983) and R. E. Taylor, *J. Vacuum Sci. Tech.* A1 1615.
9. Maleki, H. (1994) and L. R. Holland, *J. Appl. Phys.* 76 4022.
10. Sha, Yi-Gao. (1996) Ching-Hua Su, K. Mazuruk and S. L. Lehoczky, *J. Appl. Phys.* 80 752.
11. Kubaschewski, O. (1941) and F. E. Witting, *Elektrochem* 47, 433.
12. Medzhidov, R. A. (1975) and S. M. Rasulov, *Inorganic Materials* 11, 555.
13. Takeda, S. (1985) H. Okazaki and S. Tamaki, *J. Phys. Society of Japan* 54, 1890.